

# Low velocity quantum reflection of Bose-Einstein condensates

T. A. Pasquini, M. Saba, G. Jo, Y. Shin, W. Ketterle, D. E. Pritchard\*

*Department of Physics, MIT-Harvard Center for Ultracold Atoms, and Research Laboratory of Electronics,  
Massachusetts Institute of Technology, Cambridge, Massachusetts, 02139*

T. A. Savas

*NanoStructures Laboratory and Research Laboratory of Electronics,  
Massachusetts Institute of Technology, Cambridge, Massachusetts, 02139*

N. Mulders

*Department of Physics, University of Delaware, Newark, DE, 19716*

(Dated: May 8, 2018)

We studied quantum reflection of Bose-Einstein condensates at normal incidence on a square array of silicon pillars. For incident velocities of 2.5-26 mm/s observations agreed with theoretical predictions that the Casimir-Polder potential of a reduced density surface would reflect slow atoms with much higher probability. At low velocities (0.5-2.5 mm/s), we observed that the reflection probability saturated around 60% rather than increasing towards unity. We present a simple model which explains this reduced reflectivity as resulting from the combined effects of the Casimir-Polder plus mean field potential and predicts the observed saturation. Furthermore, at low incident velocities, the reflected condensates show collective excitations.

PACS numbers: 34.50.Dy, 03.75.-b, 03.75.Kk

Quantum fluctuations of the electromagnetic field exert forces on objects and are responsible for the attractive interactions between two neutral objects, e.g. an atom and a surface [1]. Such interactions are typically weak and decay rapidly with increasing separation. Still, they are important for nanoscale devices [2, 3] and when ultracold atoms are trapped close to a surface [4, 5, 6]. One spectacular consequence of the Casimir-Polder potential is the prediction of total quantum reflection of very slow atoms from neutral surfaces: atoms incident on a surface at low velocity are accelerated toward the surface so abruptly that they reflect from the potential instead of being drawn into the surface [7, 8, 9, 10]. If high reflection probabilities could be realized, new atom-optical devices such as mirrors and cavities would be possible without the need of magnetic or optical fields. However, in a recent study of quantum reflection of Bose-Einstein condensates, the reflection probability was limited to  $\sim 15\%$  at low velocity [11]. A theoretical paper simulating quantum reflection of Bose-Einstein condensates could not explain the low reflectivity [12].

In this work, we investigate the quantum reflection of Bose-Einstein condensates (BECs) from surfaces for velocities near and below 1 mm/s. To enhance quantum reflection, we use a pillared silicon surface, in the spirit of previous experiments with grazing-incidence neon atoms on ridged silicon [13, 14, 15]. We observe quantum reflection of Bose-Einstein condensates with probabilities of up to 67% for velocities of  $\sim 1$  mm/s, corresponding to a collision energy of  $k_B \times 1.5$  nK. We propose a simple model to explain how mean field interactions interfere with the reflection process and prevent the observation of higher reflection coefficients with BECs. Further, due to the

greatly enhanced reflection coefficients, we observe collective excitations of the reflected condensate and incoherent scattering between incident and reflected clouds.

Bose-Einstein condensates of  $^{23}\text{Na}$  atoms were prepared and transferred into a loosely confining gravito-magnetic trap, comprising a single coil and three external bias fields, as described in Ref. [16]. For typical loading parameters, condensates with  $N \approx 1 \times 10^6$  atoms were confined  $\sim 1$  cm above the coil in a harmonic trap characterized by angular frequencies  $(\omega_\perp, \omega_y, \omega_z) = 2\pi \times (4.2, 5.0, 8.2)$  Hz, where directions  $(\perp, y, z)$  are defined in Figure 1. At this point,  $\omega_\perp$  and  $\omega_y$  were adjusted by changing the vertical bias field as described in Ref. [16]. Typical densities in the trap were  $\sim 5 \times 10^{12} \text{ cm}^{-3}$  and diameters were  $\sim 150 \mu\text{m}$ . A silicon surface attached to a micrometric, motorized linear actuator was mounted  $\sim 1$  cm above the single coil. The position of the surface relative to the center of the coil was adjustable during the experiment as shown in Figure 1a.

The surface used in this experiment, provided by the MIT Nanostructures laboratory, was a pillar structure etched into single-crystal silicon. The structure was created by Interference Lithography (IL) and various subsequent etching steps [17, 18, 19]. Figure 1b shows the final surface as an array of  $1 \mu\text{m}$  tall,  $50 \text{ nm}$  diameter pillars spaced at  $500 \text{ nm}$ . Such a surface should provide a Casimir potential approximately 1% of the value for a solid Si surface. The quantum reflection efficiency depends inversely on the strength of the interaction, and a dilute surface is expected to exhibit enhanced reflection.

Studying the reflection properties of the surface requires a controlled collision. After loading the condensate into the trap, the surface was moved to a desired distance

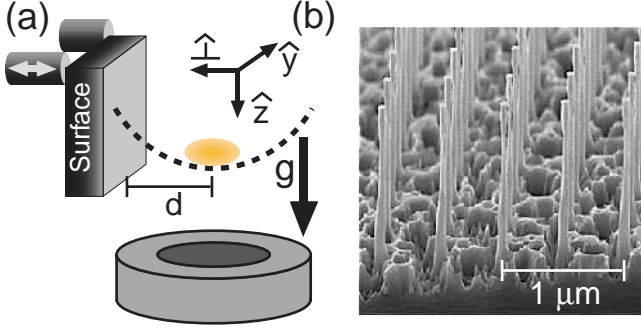


FIG. 1: Experimental schematic. (a) Atoms were confined in a gravito-magnetic trap near a pillared Si surface. Atoms were accelerated towards the surface by displacing the trapping potential a distance  $d$  (greatly exaggerated) so that it was centered on the surface. The surface was mounted on a translation stage and could be removed at any point for imaging. (b) Scanning electron micrograph of the pillared Si surface used in this experiment.

$d$  from the trap center. By changing the bias field  $B_{\perp}$  appropriately, a dipole oscillation centered on the surface was induced [11]. After waiting  $T_{\perp}/4 = 2\pi/4\omega_{\perp}$  the atoms hit the surface with velocity  $v_{\perp} = d\omega_{\perp}$ . By varying  $\omega_{\perp}$  between  $2\pi \times 2$  and  $2\pi \times 4$  Hz and  $d$  over  $50 \mu\text{m}$  to  $1 \text{ mm}$ , velocities in the range of  $0.5$  to  $26 \text{ mm/s}$  could be studied. The reflection probability was calculated as the ratio of the average reflected atom number to the average incident atom number [26]. The reflection probability, along with data previously collected for a solid silicon surface [11], are shown in Figure 2. The pillared surface shows higher reflectivity over a wider range of incident velocity, as expected. The reflection maximum is  $67\%$  for a velocity of  $1.2 \text{ mm/s}$  and reflection probabilities above  $10\%$  were measured at velocities up to  $20 \text{ mm/s}$ . Below  $\sim 3 \text{ mm/s}$ , the reflection probability flattens near  $55\%$ , qualitatively similar to the behavior of the solid surface where the reflectivity flattened near  $12\%$  in the same velocity range.

We calculated a theoretical reflection probability of a single atom from the pillared surface using three numerical simulations. The surface potentials of the Casimir-Polder form  $C_4/r^4$  are obtained using  $C_4^{Si} = 6.2 \times 10^{-56} \text{ Jm}^4$  for bulk silicon [20] and combining contributions from both the pillar layer and the bulk substrate. Reflection probabilities were calculated by numerically solving the Schrödinger equation for a 1D potential [21]. We consider three averaging schemes for simulating the experiment: (1) we average the density of the material before calculating the potential, simulating the surface as a  $1 \mu\text{m}$  thick overlayer of material with  $C_4 = 0.01 \times C_4^{Si}$  added to a semi-infinite slab of material with  $C_4 = C_4^{Si}$ , (2) we calculate the 3D potential from the pillared structure numerically by integrating over the regions of space containing material with  $C_4 = C_4^{Si}$  [22] and then average

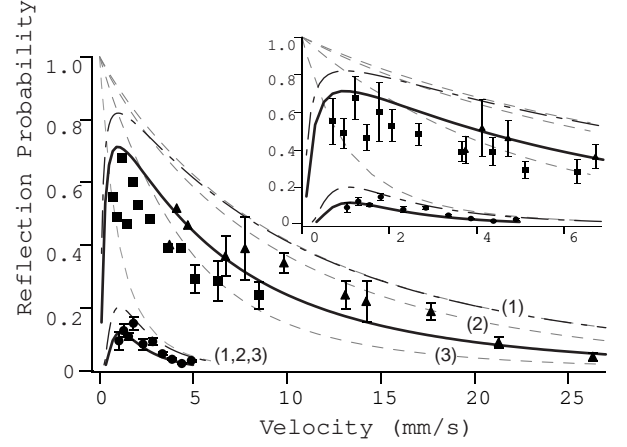


FIG. 2: Reflection probability vs incident velocity. Data were collected in a magnetic trap with trap frequencies  $2\pi \times (2.0, 2.5, 8.2) \text{ Hz}$  (squares) and  $2\pi \times (4.2, 5.0, 8.2) \text{ Hz}$  (triangles). For comparison, data from Ref. [11] for reflection off a solid silicon surface are shown as circles. Incident and reflected atom numbers were averaged over several shots. For clarity error bars for data below  $5 \text{ mm/s}$  are shown only on the inset plot, which has a different horizontal axis to emphasize the low velocity data. Systematic uncertainty in the velocity due to residual motion is approximately  $10\%$ . Theoretical curves are described in the text.

to obtain a 1D potential, or (3) we assume that atoms follow a linear trajectory toward the surface (Eikonal approximation), and calculate the reflection probability from many points above the surface before averaging the reflection probability. The resulting reflection probability curves are shown in Figure 2 as numbered dashed gray lines. The predictions of model (1) and (2) are similar for the pillared surface. They show that the reflection probability depends mainly on the the diluted pillar layer and only weakly on the bulk material underneath or the arrangement of the pillars. Model (3) should only be valid for high incident velocity, when the de Broglie wavelength  $\lambda_{dB}$  is significantly smaller than the surface structure. This is not the case in our experiment where  $\lambda_{dB} \simeq 1 \mu\text{m}$  exceeds the spacing of the pillars.

All calculations predict that the reflection probability approaches unity for low incident velocity. This is in contrast to our observation that the reflection probability saturates below  $3 \text{ mm/s}$  for both the pillared and solid surfaces. It was suggested that this saturation is due to low velocity excitations which smear out the condensate density. Although the reflectivity approaches unity, some reflected atoms would appear in a diffuse cloud which may fall below a detection threshold [12]. However, this could explain our previous results [11] only when we assume a density threshold for detection of  $0.25 \times n_0 \approx 10^{12} \text{ cm}^{-3}$ , where  $n_0$  is the central condensate density, which is twenty times higher than the lowest densities we are able to detect [16].

There is a finite-size correction to the standard descrip-

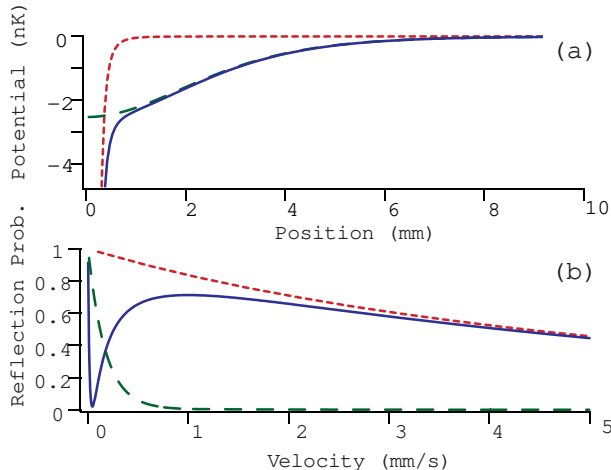


FIG. 3: Mean field model for quantum reflection of condensates. (a) The trapped condensate provides a repulsive mean-field energy which is a constant away from the surface and, within the healing length  $\xi$ , drops to zero. The dashed curve shows this mean-field potential set to zero at infinity. This potential combined with the Casimir potential (dotted), creates the composite potential (solid) which we use to model reflection in the presence of a condensate. (b) The reflection probabilities from the same the potentials for low velocities.

tion of quantum reflection, but it is too small to account for our observations. For an incident atom cloud of size  $d$ , the smallest incident velocity is  $h/md$ , approximately 0.2 mm/s for our parameters. We conclude that a single-particle description can not account for our low-velocity data and now discuss possible effects due to the condensate’s mean field interaction.

The mean field potential is taken to be that of a condensate at rest with a fully reflecting wall as a boundary condition. The condensate’s density decays towards zero at the wall over a characteristic length scale given by the healing length,  $\xi$ . The atoms at the edge of the condensate thereby acquire a velocity given by  $\approx h/m\xi$  which is approximately equal to the speed of sound  $c$ . If the healing length is much larger than the relevant range of the Casimir-Polder potential, approximately  $1 \mu\text{m}$  as defined by the so called badlands region [10], one would assume that the mean field potential simply accelerates the atoms. Atoms leaving the condensate enter the region of quantum reflection with an incident velocity obtained from  $mv^2/2 = U = mc^2$ . This model would shift the single-atom quantum reflection curves by the velocity  $v = \sqrt{2c}$  which is  $\approx 1.5 \text{ mm/s}$  for our parameters. This shift is too small to explain the low reflectivity at our lowest velocities. Additionally, the assumption that the healing length is much larger than the distance at which quantum reflection happens is not valid for our data.

In order to fully account for interaction effects, we calculate the quantum reflection probability using a composite potential which includes both the Casimir-Polder

potential and the mean field potential (Fig 3a). The results now show a dramatic reduction of the reflectivity at low velocity, as shown in Figure 3b. At high velocities ( $> 3 \text{ mm/s}$ ), quantum reflection occurs close to the surface where the mean field potential plays no role. As a result, the predictions of the composite model are similar to the single atom theory. As the velocity is reduced, the point of reflection moves outward, into the region where the mean-field potential “softens” the Casimir-Polder potential. At very low velocities ( $< 0.1 \text{ mm/s}$ ), when the badlands region is far from the surface, the predicted reflection resembles the reflection probability from the tail of the condensate rather than from the Casimir-Polder potential. We note that the model continues to predict perfect reflection at zero incident velocity, however the approach is distinctly non-monotonic; the reflection probability saturates and decreases precipitously near 1 mm/s before rising to unity. This model predicts well, without any free parameter, the velocities below which we have observed saturation of the reflectivity for both the solid and pillared surface as shown by the dot-dashed lines in Figure 2. Unfortunately, the data do not extend far enough into the low velocity regime to confirm the model’s prediction of a sharp drop at low velocity or the ultimate asymptote to unity.

The model does not include the effects of the moving condensate, its observed collective excitations, or the distortion of the condensate wavefunction by surface attraction or the loss of atoms to the surface.

The calculated curves are not in quantitative agreement with the experimental data; the observed reflection probabilities are lower, even at high velocity. One possible explanation is the further modification of the potential by stray electric fields, caused by sodium atoms deposited on the surface (adatoms). Recently, the partial ionization of rubidium adatoms by bulk silicon has been shown empirically to produce an electric field of several V/cm at  $10 \mu\text{m}$  from the surface [4]. This electric field, which falls off as  $1/r^2$ , will produce an additional potential,  $V_A(r) = -A/r^4$ , which will reduce the reflection probability. To account for stray electric fields, we fit the high velocity data for the pillared (solid) surface using a potential  $V_{tot} = -0.01 \times C_4^{Si}/r^4 - A/r^4$  ( $V_{tot} = -C_4^{Si}/r^4 - A/r^4$ ). We find for the pillared (solid) surface a value of  $A$  of  $0.02 \times C_4^{Si}$  ( $C_4^{Si}$ ) corresponding to a stray field  $\sim 10 \text{ V/cm}$  ( $\sim 100 \text{ V/cm}$ ) at  $1 \mu\text{m}$  for the pillared (solid) surface, smaller than the values measured in the rubidium experiment. If we combine the stronger surface potential with the mean-field potential we have a phenomenological model which is consistent with all our data, shown in Figure 2 as solid lines. It would be very interesting to test this model by varying the density over a large range and try to observe the predicted decrease of the saturation velocity for lower density. Unfortunately, we couldn’t study quantum reflection at lower density due to rapid decrease of the signal-to-noise ratio.

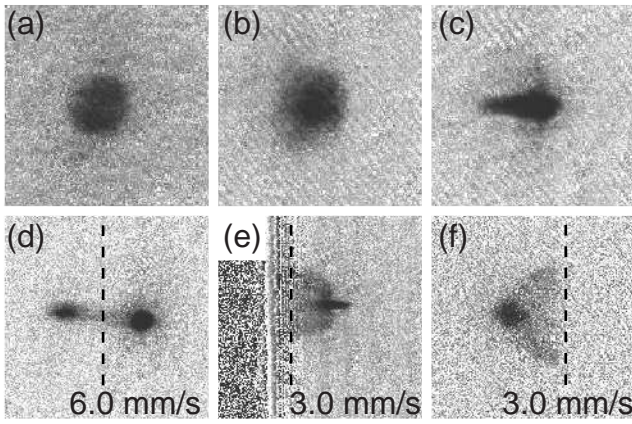


FIG. 4: Menagerie of reflection effects. (a,b,c) As the incident velocity is reduced, the reflected condensate becomes increasingly excited. (d) By removing the surface at the moment of reflection, we can see both the incident (left) and reflected (right) condensates. The reflection probability is 30%. (e) The collision of the incident and reflected condensates produces a strong s-wave scattering halo at low velocity, visible here  $T_{\perp}/4$  after reflection. The surface is still present on the left in this image. Half of the halo is missing due to surface reflection or absorption. (f) With the surface removed, the scattered atoms remain in the trap after an additional half trap period, and appear reversed in position and velocity. Field of view for images a, b, c is  $540 \mu\text{m}$  and for d, e, f is  $800 \mu\text{m}$ ; the dashed line is the position of the surface (moved for imaging) at the moment of reflection.

The higher reflection efficiency of the pillared surface in excess of 50% allowed us to study other aspects of quantum reflection of condensates at low velocity. Because of the finite size of the condensate, a standing wave is present in the condensate during the collision time which is inversely proportional to the incident velocity. As this time becomes comparable to the transverse and vertical trap periods, vortex rings, solitons, and other excitations may form, distorting the cloud [12]. In our experiment, this velocity is approximately  $2\text{mm/s}$ . At high velocities ( $> 4\text{mm/s}$ ), we observe that the reflected condensate appears, apart from diminished size and number, similar to the incident condensate. A condensed fraction and a thermal population, both present in the initial cloud are also present in the reflected cloud, shown in Figure 4a. As the incident velocity is reduced, as in Fig. 4b and c, the cloud develops a complex surface mode excitation [27].

Furthermore, we observe elastic s-wave scattering between atoms in the incident and reflected condensates. S-wave scattering redistributes atoms in two colliding clouds with initial relative wavevector  $\vec{k}$  evenly onto a sphere of radius  $|\vec{k}|$  [23, 24]; an image of the atoms taken after a hold time  $T_{\perp}/4$  will show the two clouds on opposite sides of the scattering sphere. In the present experiment, the reflected front part of the condensate collided with the still incident tail part (Fig. 4d). The scattering

halo was observed after sufficient hold time (Fig. 4 e,f).

We also performed the experiment using an aerogel surface. Aerogels are electrically insulating, randomly structured, silica foams with a density of  $\sim 2\%$  of bulk silica [25] and should display reflection properties similar to the pillared surface. We were unable to observe quantum reflection above our detection threshold of  $\sim 2\%$ , an effect we attribute to uncontrolled patch charges which strongly distort the Casimir-Polder potential and prevent efficient reflection.

In light of the strong increase in reflection probability for the pillared structure, we want to discuss the ultimate limits of quantum reflection probability for condensates. We have found strong evidence that the presence of a condensate will distort the potential and prevent efficient reflection at low velocity. Our simple model predicts improvements for longer healing lengths. Unfortunately, the corresponding reduction in condensate density would be a severe limit for atom optical devices based on quantum reflection. Another way to improve the reflectivity is by further reducing the density of the surface. Certainly it is possible to increase the pillar spacing. However, such widely spaced pillars will only dominate the potential if their height is simultaneously increased, which is beyond the limit of current fabrication techniques. Similarly, narrower pillars may be possible, but not with the height required to dominate the potential.

This work was supported by NSF, ONR, ARO, DARPA, and NASA. We thank S. Will for experimental assistance, M. Zwierlein for suggestions about the experiment and R. Scott and M. Fromhold for useful discussions.

---

\* URL: [http://cua.mit.edu/ketterle\\_group/](http://cua.mit.edu/ketterle_group/)

- [1] H. B. G. Casimir and P. Polder, Phys. Rev. **73**, 360 (1948).
- [2] M. Bordag, U. Mohideen, and V. M. Mostepanenko, Phys. Rep. **353**, 1 (2001).
- [3] H. B. Chan et al., Science **291**, 1941 (2001).
- [4] J. M. McGuirk et al., Phys. Rev. A **69**, 062905 (2004).
- [5] D. M. Harber et al., J. Low. Temp. Phys. **133**, 229 (2003).
- [6] Y. Lin et al., Phys. Rev. Lett. **92**, 050404 (2004).
- [7] D. P. Clougherty and W. Kohn, Phys. Rev. B **46**, 4921 (1992).
- [8] C. Carraro and M. W. Cole, Prog. Surf. Sci. **57**, 61 (1998).
- [9] A. Mody et al., Phys. Rev. B **64**, 085418 (2001).
- [10] H. Friedrich, G. Jacoby, and C. G. Meister, Phys. Rev. A **65**, 032902 (2002).
- [11] T. A. Pasquini et al., Phys. Rev. Lett. **93**, 223201 (2004).
- [12] R. G. Scott et al., Phys. Rev. Lett. **95**, 073201 (2005).
- [13] F. Shimizu and J. Fujita, J. Phys. Soc. Japan **71**, 5 (2002).
- [14] H. Oberst et al., Phys. Rev. Lett. **94**, 013203 (2005).
- [15] D. Kouznetsov and H. Oberst, Phys. Rev. A **72**, 013617 (2005).

- [16] A. E. Leanhardt et al., *Science* **301**, 1513 (2003).
- [17] H. I. Smith et al., *J. Vac. Sci. Technol. B* **9**, 2992 (1991).
- [18] M. L. Schattenburg, R. J. Aucoin, and R. C. Fleming, *J. Vac. Sci. Technol. B* **13**, 3007 (1995).
- [19] T. A. Savas et al., *J. Vac. Sci. Technol. B* **14**, 4167 (1996).
- [20] Z. C. Yan, A. Dalgarno, and J. F. Babb, *Phys. Rev. A* **55**, 2882 (1997).
- [21] F. Shimizu, *Phys. Rev. Lett.* **86**, 987 (2001).
- [22] P. W. Milonni and M.-L. Shih, *Phys. Rev. A* **45**, 4241 (1992).
- [23] K. Gibble, S. Chang, and R. Legere, *Phys. Rev. Lett.* **75**, 2666 (1995).
- [24] A. P. Chikkatur et al., *Phys. Rev. Lett.* **85**, 483 (2000).
- [25] J. Fricke and A. Emmerling, *J. Am. Ceram. Soc.* **8**, 2027 (1992).
- [26] Atom numbers were obtained by exposing the atoms to a light pulse which transferred atoms from the state  $|F = 1\rangle$  to  $|F = 2\rangle$ . After a wait time of  $\sim 2$  ms to allow optically dense regions of the cloud to expand, the distributions were imaged using the  $|F = 2\rangle$  to  $|F = 3\rangle$  cycling transition. Expansion by photon recoil distorts the distribution, but gives accurate relative numbers.
- [27] A movie of reflection at 3 mm/s is available at [http://cua.mit.edu/ketterle\\_group/Animation\\_folder/QRMovie.wmv](http://cua.mit.edu/ketterle_group/Animation_folder/QRMovie.wmv).